Inorg. Chem. **2009**, *48*, 1250−1256

Structural Models for the Active Site of Acetyl-CoA Synthase: Synthesis of Dinuclear Nickel Complexes Having Thiolate, Isocyanide, and Thiourea on the Ni_p Site

Mikinao Ito, Mai Kotera, Yumei Song, Tsuyoshi Matsumoto, and Kazuyuki Tatsumi*

Research Center for Materials Science, and Department of Chemistry, Graduate School of Science, Nagoya University, Furo-cho, Chikusa-ku, Nagoya 464-8602, Japan

Received October 15, 2008

The trinuclear nickel complex [{Ni(dadt^{Et})}$_2$Ni](NiBr$_4$) (dadt^{Et} = *N,N'*-diethyl-3,7-diazanonane-1,9-dithiolate) (**1a**), prepared by the reaction of Ni(dadt^{Et}) and Ni(EtOH)$_4$Br$_2$, was found to serve as a useful synthetic precursor of various dinuclear nickel complexes modeling the active site of acetyl-CoA synthase (ACS). The reactions of **1a** with 4 equiv of the potassium salts of arenethiolates in ethanol produced a series of dinuclear nickel thiolate complexes Ni(dadt^{Et})Ni(SAr)$_2$ (Ar = Ph (**2a**), *p*-Tol (**2b**), 2,4,6-triisopropylphenyl (Tip) (**2c**)) in good yields. The analogous reactions of **1a** with Ag(OTf) in the presence of ^{t}BuNC and (NMe$_2$)$_2$CS (tmtu) generated the dicationic dinuclear nickel complexes [Ni(dadt^{Et})Ni(^{t}BuNC)$_2$](OTf)$_2$ (**3**) and [Ni(dadt^{Et})Ni(tmtu)$_2$](OTf)$_2$ (**4**), respectively. The molecular structures of **1a**, **2a**−**c**, **3**, and **4** determined by X-ray analysis compare well with that of A-cluster in ACS.

Introduction

Acetyl-CoA synthase (ACS)/CO dehydrogenase (CODH) is an unique multifunctional enzyme, playing an important role in the Wood−Ljungdahl pathway of CO_2 fixation.[1] While CODH catalyzes the reversible reduction of CO_2 to CO, ACS assembles acetyl-CoA from carbon monoxide, coenzyme A, and a methyl moiety derived from the corrinoid iron−sulfur protein (CFeSP). Recently the crystal structures of the ACS/CODH system from the bacteria *Moorella thermoacetica* have been determined.[2,3] The ACS active site, denoted as the A-cluster, consists of a dinuclear nickel site and a Fe_4S_4 cubane cluster formulated as [Ni$_d$\{(μ-Cys-S)-Gly-(μ-Cys-S)\}Ni$_p$(X)](μ-Cys-S)\{Fe$_4$(μ-Cys-S)$_3$S$_4$\} (Figure 1), where the two nickel atoms are designated as Ni_d and Ni_p, being *distal* and *proximal* to the Fe_4S_4 cluster, respectively. The Ni_d site is square planar, coordinated by two cysteine sulfurs and two amide nitrogens of the Cys-Gly-Cys tripeptide from the protein backbone. The two cysteine sulfurs of this tripeptide also bind Ni_p, along with cysteine thiolate from the [Fe_4S_4] cluster and an unidentified ligand X.[3] Although crystal structures containing Cu(I)[2] and Zn(II)[3] at the proximal site have also been reported, recent evidence is convincing that a nickel ion at the proximal is essential for enzymatic activity.[4] The monofunctional ACS isolated from *Carboxydothermus hydrogenoformans* also contains Ni_p.[5]

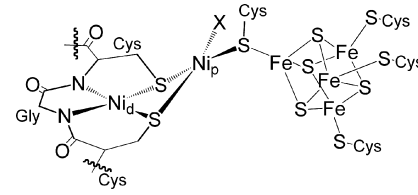

Figure 1. Drawing of the ACS active site structure.

* To whom correspondence should be addressed. E-mail: i45100a@nucc.cc.nagoya-u.ac.jp.

(1) (a) Lindahl, P. A.; Graham, D. E. In *Nickel and Its Surprising Impact in Nature*; Sigel, A., Sigel, H., Sigel, R. K. O., Eds.; John Wiley & Sons, Ltd.: Chichester, U.K., 2007; Metal Ions in Life Science, Vol. 2, Chapter 9, pp 357−411. (b) Ragsdale, S. W. *Crit. Rev. Biochem. Mol. Biol.* **2004**, *39*, 165–195. (c) Riordan, C. G. *J. Biol. Inorg. Chem.* **2004**, *9*, 509–510.

(2) Doukov, T.; Iverson, T. M.; Seravalli, J.; Ragsdale, S. W.; Drennan, C. L. *Science* **2002**, *298*, 567–572.

(3) Darnault, C.; Volbeda, A.; Kim, E. J.; Legrand, P.; Vernede, X.; Lindahl, P. A.; Fontecilla-Camps, J. C. *Nat. Struct. Biol.* **2003**, *10*, 271–279.

(4) (a) Bramlett, M. R.; Tan, A.; Lindahl, P. A. *J. Am. Chem. Soc.* **2003**, *125*, 9316–9317. (b) Seravalli, J.; Xiao, Y.; Gu, W.; Cramer, S. P.; Antholine, W. E.; Krymov, V.; Gerfen, G. J.; Ragsdale, S. W. *Biochemistry* **2004**, *43*, 3944–3955.

(5) Svetlitchnyi, V.; Dobbek, H.; Meyer-Klaucke, W.; Meins, T.; Thiele, B.; Römer, P.; Huber, R.; Meyer, O. *Proc. Natl. Acad. Sci. U.S.A.* **2004**, *101*, 446–451.

10.1021/ic801967e CCC: $40.75
Published on Web 01/07/2009

Since the elucidation of the ACS crystal structure, the synthesis of the A-cluster model complex has been a challenge for the bioinorganic chemists. The typical synthetic method for modeling the dinuclear nickel active site reported so far involves the reaction of square-planar Ni(N_2S_2) complexes mimicking the Ni_d site with exogenous nickel complexes bearing appropriate labile ligands. The N_2S_2 ligands are diaminedithiolates such as *N,N'*-diethyl-3,7-diazanonane-1,9-dithiolate (dadt^{Et}) or diamidodithiolates such as 2,7-dioxo-3,6-diazaoctanedithiolate (ema) and a Cys-Gly-Cys tripeptide (CGC).[6,7] However, the ligand lability for the exogenous nickels often leads to the formation of trinuclear complexes of the type {Ni(N_2S_2)}$_2$Ni.[6,7a−e] Thus, the nickel complexes containing chelate diphos or terpyridine ligands have been used as the exogenous nickel sources to stabilize the dinuclear nickel complexes such as Ni(CGC)Ni(L) (L = depe or dppe),[7a] Ni(L-655)Ni(depe),[7b] Ni(NpPepS)Ni(L) (NpPepS = *N,N'*-napthalenebis(*o*-mercaptobenzamide), L = terpy or dppe),[7e] [Ni(dadt^{Et})Ni(dppe)]$^{2+}$,[7f] and [Ni(Phma)Ni(dppe)Me]$^+$.[7g] Although these complexes model the dinuclear nickel core of ACS, the rigid coordination of the Ni_p by the multidentate ligands may interfere with binding the substrates such as CO, Me, and thiolate in the development of ACS model reaction. There is one example of the dinuclear nickel model having an appended thiolate on the Ni_p site, [Ni(dadt^{Et})Ni($SCH_2CH_2PPh_2$)][PF_6] reported by Holm,[7c] while in the A-cluster the Ni_p is bridged with the cysteine thiolates of Ni(N_2S_2) unit and coordinated with an appended third cysteine thiolate arising from a [Fe_4S_4] cluster. Besides, we also recall the bimetallic Ni(II)−Ni(0) CO complex, Ni(S_2N_2')Ni(CO)$_2$, reported by Rauchfuss, which is the first structurally characterized complex as a possible reduced-ACS active site model.[8]

Herein we report the synthesis of a series of dinuclear nickel complexes, Ni(dadt^{Et})Ni(SAr)$_2$ (Ar = Ph, *p*-Tol, 2,4,6-triisopropylpheny (Tip)) and [Ni(dadt^{Et})NiL_2]$^{2+}$ (L = ^{t}BuNC, tmtu), from the preformed trinuclear nickel cluster [{Ni(dadt^{Et})}$_2$Ni]($NiBr_4$). These dinuclear nickel complexes having the monodentate thiolates and donors represent new models for the ACS active site.

Experimental Section

General Procedures. All reactions and manipulations were conducted using standard Schlenk and vacuum line techniques or in a glovebox under a nitrogen atmosphere. Hexane, ether, tetrahydrofuran (THF), acetonitrile, and toluene were purified according to the method described by Grubbs, in which the solvents were passed over columns of activated alumina and copper catalyst supplied by Hansen & Co. Ltd. Dichloromethane was distilled from CaH_2. Methanol and ethanol were distilled from magnesium turnings. Deuterated solvents were dried over potassium (THF-d_8), sodium (benzene-d_6), CaH_2 (acetonitrile-d_3, dichloromethane-d_2, chloroform-*d*) or molecular sieves 4 Å (dimethylsulfoxide-d_6) under nitrogen. ^{1}H NMR spectra were recorded on a JEOL ECA-600. IR spectra were measured on a JASCO FT/IR-410 spectrometer. UV/vis spectra were recorded in 10 mm quarz glass cells on a JASCO V-560 spectrometer. Electrospray ionization time-of-flight mass spectrometry (ESI-TOF-MS) spectra were obtained from a Micromass LCT TOF-MS spectrometer. Fast atom bombardment (FAB) mass spectra were obtained on a JEOL JMS-LCMATE mass spectrometer under the stream of high energy Xe gas, where 3-nitrobenzyl alcohol was used as the matrix. Elemental analyses were recorded on a LECO-CHNS-932 elemental analyzer where the crystalline samples were sealed in silver capsules under nitrogen. The compounds Ni(dadt^{Et}),[9] Ni(EtOH)$_4$Br$_2$,[10] [Et_4N]$_2$[Ni(S-*p*-Tol)$_4$],[11] and TipSH (Tip = 2,4,6-triisopropylphenyl)[12] were prepared according to literature procedures.

Synthesis of [{Ni(dadt^{Et})}$_2$Ni][$NiBr_4$] (1a). When an ethanol solution (30 mL) of Ni(EtOH)$_4$Br$_2$ (4.00 g, 9.93 mmol) was added to a solution of Ni(dadt^{Et}) (3.06 g, 9.96 mmol) in ethanol (100 mL) at room temperature, a dark green crystalline solid precipitated. After stirring the suspension overnight, this solid was separated by filtration and dried in vacuo to give **1a** (4.35 g, 83% yield) as a dark green crystalline powder. Crystallization from acetonitrile/ether gave crystals suitable for X-ray structural analysis. ESI-MS (CH_3CN): m/z = 335.9 (M^{2+}). Anal. Calcd for $C_{22}H_{48}Br_4N_4Ni_4S_4$: C, 25.29; H, 4.635; N, 5.367. Found: C, 24.78; H, 4.603; N, 5.272. μ_{eff} = 0.5 μ_B in CD_3OD, according to the NMR method described by Evans;[13] a solution of **1a** (10.0 mg) in CD_3OD was prepared in a 1.0 mL volumetric flask. A portion of this solution was transferred into a capillary tube that was sealed and dropped into a NMR tube containing CD_3OD. The chemical shift difference of the tetramethylsilane signal between the inner and the outer tubes was measured at room temperature. From the difference in the chemical shifts the μ_{eff} value was calculated. ^{1}H NMR (CD_3OD solution of **1a**)[14] δ 3.46−3.38 (br m, 2H, NCH_2CH_2S), 3.23 (dq, J = 6.9 Hz, 14.0 Hz, 2H, CH_3CH_2), 3.11 (dq, J = 6.9 Hz, 14.0 Hz, 2H, CH_3CH_2), 2.99−2.91 (m, 4H, $NCH_2CH_2CH_2N$), 2.62 (dd, J = 8.5 Hz, 3.0 Hz, 2H, NCH_2CH_2S), 2.19−2.13 (m, 1H, $NCH_2CH_2CH_2N$), 2.16 (dd, J = 8.5 Hz, 3.0 Hz, 2H, NCH_2CH_2S), 2.01−1.93 (m, 1H, $NCH_2CH_2CH_2N$), 2.13−2.05 (br m, 2H, NCH_2CH_2S), 1.41 (t, J = 6.9 Hz, 6H, CH_3CH_2). UV/vis (DMSO solution of **1a**):[14] λ_{max}/

(6) (a) Golden, M. L.; Rampersad, M. V.; Reibenspies, J. H.; Darensbourg, M. Y. *Chem. Commun.* **2003**, 1824–1825. (b) Amoroso, A. J.; Chung, S. S. M.; Spencer, D. J. E.; Danks, J. P.; Glenny, M. W.; Blake, A. J.; Cooke, P. A.; Wilson, C.; Schröder, M. *Chem. Commun.* **2003**, 2020–2021. (c) Harrop, T. C.; Olmstead, M. M.; Mascharak, P. K. *Chem. Commun.* **2004**, 1744–1745. (d) Golden, M. L.; Jeffery, S. P.; Miller, M. L.; Reibenspies, J. H.; Darensbourg, M. Y. *Eur. J. Inorg. Chem.* **2004**, 231–236. (e) HatlevikØ.; Blanksma, M. C.; Mathrubootham, V.; Arif, A. M.; Hegg, E. L. *J. Biol. Inorg. Chem.* **2004**, *9*, 238–246.

(7) (a) Krishnan, R.; Riordan, C. *J. Am. Chem. Soc.* **2004**, *126*, 4484–4485. (b) Rao, P. V.; Bhaduri, S.; Jiang, J.; Holm, R. H. *Inorg. Chem.* **2004**, *43*, 5833–5849. (c) Rao, P. V.; Bhaduri, S.; Jiang, J.; Hong, D.; Holm, R. H. *J. Am. Chem. Soc.* **2005**, *127*, 1933–1945. (d) Duff, S. E.; Barclay, J. E.; Davies, S. C.; Evans, D. J. *Inorg. Chem. Commun.* **2005**, *8*, 170–173. (e) Harrop, T. C.; Olmstead, M. M.; Mascharak, P. K. *Inorg. Chem.* **2006**, *45*, 3424–3436. (f) Wang, Q.; Blake, A. J.; Davies, E. S.; McInnes, E. J. L.; Wilson, C.; Schröder, M. *Chem. Commun.* **2003**, 3012–3013. (g) Dougherty, W. G.; Rangan, K.; O'Hagan, M. J.; Yap, G. P. A.; Riordan, C. G. *J. Am. Chem. Soc.* **2008**, *130*, 13510–13511.

(8) Linck, R. C.; Spahn, C. W.; Rauchfuss, T. B.; Wilson, S. R. *J. Am. Chem. Soc.* **2003**, *125*, 8700–8701.

(9) Osterloh, F.; Saak, W.; Pohl, S. *J. Am. Chem. Soc.* **1997**, *119*, 5648–5656.

(10) Ward, L. G. L. *Inorg. Synth.* **1971**, *13*, 154.

(11) Rosenfield, S. G.; Armstrong, W. H.; Mascharak, P. K. *Inorg. Chem.* **1986**, *25*, 3014–3018.

(12) Blower, P. J.; Dilworth, J. R.; Hutchinson, J. P.; Zubieta, J. A. *J. Chem. Soc., Dalton Trans.* **1985**, 1533–1541.

(13) (a) Evans, D. F. *J. Chem. Soc.* **1959**, 2003–2005. (b) Evans, D. F.; Fazakerley, G. V.; Phillips, R. F. *J. Chem. Soc. A* **1971**, 1931–1934. (c) Crawford, T. H.; Swanson, J. *J. Chem. Educ.* **1971**, *48*, 382–386. (d) Grant, D. H. *J. Chem. Educ.* **1995**, *72*, 39–40.

(14) The ^{1}H NMR and UV/vis data were collected for the solutions of **1a**. However, **1a** could be in equilibrium with {Ni(dadt^{Et})}$NiBr_2$ in the solutions (see Results and Discussion).

nm (ε) = 482 (sh, 3.3 × 10^2), 425 (5.7 × 10^2), 301 (sh, 1.7 × 10^4), 283 (2.3 × 10^4).

Synthesis of [{Ni(dadt^{Et})}$_2$Ni][PF$_6$]$_2$ (1b). To a methanol solution of **1a** (300 mg, 0.285 mmol) was added a methanol solution of $NaPF_6$ (100 mg, 0.595 mmol) at room temperature. The dark gray material was separated by filtration, washed with methanol, and dried in vacuo to give **1b** (270 mg, 98% yield) as a dark gray powder. ^{1}H NMR (DMSO-d_6): δ 3.48−3.32 (m, 2H, CH_3CH_2), 3.30−3.20 (m, 2H, CH_3CH_2), 2.84−2.54 (m, 8H, NCH_2-CH_2S+NCH_2CH_2S), 2.36−1.86 (m, 2H, N$CH_2CH_2CH_2$N), 1.70−1.48 (m, 2H, $NCH_2CH_2CH_2$N), 1.10−0.80 (m, 8H, CH_3CH_2+NCH_2-CH_2CH_2N). Anal. Calcd for $C_{22}H_{48}F_{12}N_4Ni_3P_2S_4$: C, 27.44; H, 5.024; N, 5.818. Found: C, 27.61; H, 4.942; N, 5.933.

Synthesis of Ni(dadt^{Et})Ni(SPh)$_2$ (2a). To an ethanol suspension (5 mL) of **1a** (50 mg, 0.048 mmol) was added a solution of KSPh (28 mg, 0.19 mmol) in ethanol (5 mL) at room temperature. The reddish brown suspension was stirred overnight. The supernatant liquid was removed, and the residue was extracted with dichloromethane (10 mL). The solution was evaporated to give **2a** (51 mg, 91% yield) as a reddish brown powder. Crystallization from dichloromethane/hexane gave crystals suitable for X-ray structural analysis. ^{1}H NMR (DMSO-d_6): δ 7.76−7.70 (m, 4H, Ph), 6.96−6.90 (m, 4H, Ph), 6.86−6.80 (m, 2H, Ph), 3.36 (dt, J = 8.5 Hz, 3.0 Hz, 2H, NCH_2CH_2S), 3.24 (dq, J = 6.9 Hz, 14.0 Hz, 2H, CH_3CH_2), 3.05 (dq, J = 6.9 Hz, 14.0 Hz, 2H, CH_3CH_2), 2.78 (dd, J = 8.5 Hz, 3.0 Hz, 2H, NCH_2CH_2S), 2.64−2.52 (m, 4H, N$CH_2CH_2CH_2$N), 1.96−1.78 (m, 2H, $NCH_2CH_2CH_2$N), 1.58 (dd, J = 8.5 Hz, 3.0 Hz, 2H, NCH_2CH_2S), 1.38 (dt, J = 8.5 Hz, 3.0 Hz, 2H, NCH_2CH_2S), 0.99 (t, J = 6.9 Hz, 6H, CH_3CH_2). Anal. Calcd for $C_{23}H_{34}N_2Ni_2S_4$: C, 47.29; H, 5.866; N, 4.795. Found: C, 47.30; H, 5.607; N, 4.416. UV/vis (DMSO): λ_{max}/nm (ε) = 520 (sh, 2.4 × 10^2), 394 (7.6 × 10^2), 327 (sh, 2.9 × 10^4), 303 (3.2 × 10^4).

Synthesis of Ni(dadt^{Et})Ni(S-*p*-Tol)$_2$ (2b). Method A. A similar procedure as used for **2a** but using KS-*p*-Tol gave **2b** in 62% yield as reddish brown crystals. ^{1}H NMR (DMSO-d_6): δ 7.60−7.54 (m, 4H, *p*-Tol), 6.76−6.70 (m, 4H, *p*-Tol), 3.36 (dt, J = 8.5 Hz, 3.0 Hz, 2H, NCH_2CH_2S), 3.22 (dq, J = 6.9 Hz, 14.0 Hz, 2H, CH_3CH_2), 3.04 (dq, J = 6.9 Hz, 14.0 Hz, 2H, CH_3CH_2), 2.78 (dd, J = 8.5 Hz, 3.0 Hz, 2H, NCH_2CH_2S), 2.64−2.54 (m, 4H, $NCH_2CH_2CH_2$N), 2.11 (s, 6H, *p*-Tol), 1.96−1.78 (m, 2H, $NCH_2CH_2CH_2$N), 1.58 (dd, J = 8.5 Hz, 3.0 Hz, 2H, NCH_2CH_2S), 1.38 (dt, J = 8.5 Hz, 3.0 Hz, 2H, NCH_2CH_2S), 1.00 (t, J = 6.9 Hz, 6H, CH_3CH_2). Anal. Calcd for $C_{25}H_{38}N_2Ni_2S_4$: C, 49.05; H, 6.256; N, 4.576. Found: C, 48.74; H, 6.393; N, 5.105. UV/vis (DMSO): λ_{max}/nm (ε) = 540 (sh, 1.0 × 10^2), 400 (7.6 × 10^3), 328 (sh, 1.4 × 10^4), 290 (1.9 × 10^4), 287 (2.0 × 10^4).

Method B. To an acetonitrile solution (10 mL) of **1b** (100 mg, 0.095 mmol) was added a solution of [Et$_4$N]$_2$[Ni(S-*p*-Tol)$_4$] (85 mg, 0.10 mmol) in acetonitrile (10 mL) at room temperature. The reddish brown solution was stirred for 12 h and evaporated in vacuo. The solid was extracted with dichloromethane (15 mL), and the solution was evaporated to dryness. The residue was washed with THF (5 mL) and methanol (10 mL) and dried in vacuo to give **2b** (92 mg, 73% yield).

Method C. To an acetonitrile solution (10 mL) of **1b** (100 mg, 0.095 mmol) was added a solution of [Et$_4$N](S-*p*-Tol) (53 mg, 0.21 mmol)) in acetonitrile (10 mL) at room temperature. After stirring for 12 h, the solution was evaporated to dryness and the residue was extracted with dichloromethane (15 mL). The solution was evaporated to dryness, and the residue was washed with methanol (10 mL) and dried in vacuo to give **2b** (55 mg, 96% yield).

Synthesis of Ni(dadt^{Et})Ni(STip)$_2$ (2c). A similar procedure as used for **2a** but using KSTip gave **2c** in 65% yield as reddish brown crystals. ^{1}H NMR (C_6D_6): δ 7.24 (s, 4H, Tip), 5.57 (sep, J = 6.8 Hz, 4H, Tip), 3.75 (dt, J = 12.0 Hz, 4.0 Hz, 2H, NCH_2CH_2S), 2.96 (sep, J = 6.8 Hz, 2H, Tip), 2.49 (dq, J = 6.9 Hz, 14.0 Hz, 2H, CH_3CH_2), 2.18 (dq, J = 6.9 Hz, 14.0 Hz, 2H, CH_3CH_2), 2.04 (dd, J = 12.0 Hz, 4.0 Hz, 2H, NCH_2CH_2S), 1.96−1.90 (m, 2H, N$CH_2CH_2CH_2$N), 1.70 (d, J = 6.8 Hz, 24H, Tip), 1.62 (dd, J = 12.0 Hz, 4.0 Hz, 2H, NCH_2CH_2S), 1.50−1.44 (m, 2H, N$CH_2CH_2CH_2$N), 1.40 (d, J = 6.8 Hz, 12H, Tip), 1.17−1.06 (m, 1H, $NCH_2CH_2CH_2$N), 0.85 (dt, J = 12.0 Hz, 4.0 Hz, 2H, NCH_2CH_2S), 0.66−0.58 (m, 1H, $NCH_2CH_2CH_2$N), 0.21 (t, J = 6.9 Hz, 6H, CH_3CH_2). Anal. Calcd for $C_{41}H_{70}N_2Ni_2S_4$: C, 58.86; H, 8.433; N, 3.348. Found: C, 59.19; H, 7.754; N, 3.445.

Synthesis of [Ni(dadt^{Et})Ni(CN^{t}Bu)$_2$](OTf)$_2$ (3). To a methanol solution (30 mL) of **1a** (300 mg, 0.285 mmol) was added ^{t}BuNC (0.13 mL, 1.2 mmol) at room temperature. The solution was stirred for 1 h, and then AgOTf (293 mg, 1.14 mmol) was added at room temperature. The red suspension was stirred for 1 h. The suspension was evaporated to dryness, and the residue was extracted with dichloromethane (50 mL). The solution was evaporated to dryness, and the residue was washed with ether to give **3** (303 mg, 64% yield) as a red powder. The crystallization from dichloromethane/hexane gave crystals suitable for X-ray structural analysis. ^{1}H NMR ($CDCl_3$): δ 3.81−3.74 (m, 2H, NCH_2CH_2S), 3.33 (dq, J = 6.9 Hz, 14.0 Hz, 2H, CH_3CH_2), 3.24 (dq, J = 6.9 Hz, 14.0 Hz, 2H, CH_3CH_2), 3.19−3.13 (m, 2H, NCH_2CH_2S), 2.94−2.88 (m, 2H, NCH_2CH_2S), 2.50−2.46 (m, 2H, NCH_2CH_2S), 2.32−2.24 (m, 4H, N$CH_2CH_2CH_2$N), 1.90−1.85 (m, 2H, $NCH_2CH_2CH_2$N), 1.60 (s, 18H, ^{t}Bu), 1.26 (t, J = 6.9 Hz, 6H, CH_3CH_2). ESI-MS (CH_2Cl_2): m/z = 679.3 ([M^{2+}+$(OTf)^-$]$^+$). IR (CH_2Cl_2): ν(CN)/cm^{-1} 2228(s), 2219(s). Anal. Calcd for $C_{23}H_{42}F_6N_4Ni_2O_6S_4$: C, 33.27; H, 5.100; N, 6.748. Found: C, 32.62; H, 4.752; N, 6.795.

Synthesis of Ni(dadt^{Et})Ni(tmtu)$_2$](OTf)$_2$ (4). To a methanol solution (30 mL) of **1a** (1.00 g, 0.951 mmol) was added tetramethylthiourea (503 mg, 3.80 mmol) at room temperature. The solution was stirred for 1 h, and then AgOTf (1.00 g, 3.89 mmol) was added at room temperature. The dark purple suspension was stirred for a day. The suspension was evaporated to dryness, and the residue was extracted with dichloromethane (50 mL). The solution was evaporated to dryness, and the residue was washed with THF to give **4** (965 mg, 53% yield) as a dark purple powder. Crystals suitable for X-ray structural analysis were obtained by crystallization of the powder from acetonitrile/ether. ^{1}H NMR (CD_3CN): δ 3.37−3.32 (m, 2H, NCH_2CH_2S), 3.16 (dq, J = 7.2 Hz, 14.0 Hz, 2H, CH_3CH_2), 3.07 (s, 24H, tmtu), 3.06 (dq, J = 7.2 Hz, 14.0 Hz, 2H, CH_3CH_2), 2.90−2.82 (m, 4H, NCH_2CH_2S), 2.56−2.52 (m, 2H, NCH_2CH_2S), 2.05−1.99 (m, 4H, N$CH_2CH_2CH_2$N), 1.87−1.81 (m, 2H, $NCH_2CH_2CH_2$N), 1.32 (t, J = 7.2 Hz, 6H, CH_3CH_2). Anal. Calcd for $C_{23}H_{48}F_6N_6Ni_2O_6S_6$: C, 29.75; H, 5.211; N, 9.052. Found: C, 29.78; H, 5.124; N, 8.790.

X-ray Structure Determinations. Crystal data and refinement parameters for the structurally characterized complexes are summarized in Table 1. Single crystals were mounted on a loop using oil (CryoLoop, Immersion Oil type B: Code 1248, Hampton Laboratories, Inc.). Diffraction data were collected at −100 °C under a cold nitrogen stream on a Rigaku AFC8 equipped with a Mercury CCD area detector (for **1a**, **2c**, **3**, and **4**) or a Rigaku RA-Micro007 with a Saturn 70 CCD area detector (for **2a** and **2b**), equipped with a graphite monochromatized Mo Kα source (λ = 0.71070 Å). Data were collected on 1200 oscillation images with an oscillation range of 0.3°. The frame data were integrated and corrected for absorption using the Rigaku/MSC CrystalClear program package. The structures were solved by direct methods (SIR-92 or SIR-97) and were refined by full-matrix least-squares

Table 1. Crystallographic Data for Complexes

	1a	2a	2b	2c	3·CH_2Cl_2	4
formula	$C_{22}H_{48}N_4S_4Br_4Ni_4$	$C_{23}H_{29}N_2S_4Ni_2$	$C_{25}H_{38}N_2S_4Ni_2$	$C_{41}H_{70}N_2S_4Ni_2$	$C_{23}H_{42}N_4S_4O_6F_6Ni_2 \cdot CH_2Cl_2$	$C_{23}H_{48}N_6S_6\ F_6Ni_2$
Fw	1051.30	579.14	612.23	836.66	915.17	928.42
crystal system	triclinic	triclinic	monoclinic	monoclinic	monoclinic	triclinic
space group	$P\bar{1}$	$P\bar{1}$	$P2_1/n$	$P2_1/n$	$P2_1/n$	$P\bar{1}$
a, Å	10.7952(16)	10.4260(14)	12.112(8)	11.765(4)	8.7723(16)	12.3351(1)
b, Å	11.1407(18)	11.0774(16)	11.209(7)	24.221(8)	19.147(4)	12.5861(1)
c, Å	15.375(2)	11.8118(19)	20.902(14)	15.828(6)	22.968(4)	14.0789(1)
α, deg	105.9193(19)	82.957(7)				69.447(6)
β, deg	93.8777(15)	78.296(6)	102.783(10)	106.781(5)	93.4050(19)	82.509(7)
γ, deg	98.975(2)	71.586(5)				68.182(7)
V, Å^3	1744.5(5)	1264.9(3)	2768(3)	4318(3)	3851.1(12)	1900.03(12)
Z	2	2	4	4	4	2
D_{calcd}, g/cm^3	2.001	1.520	1.469	1.287	1.578	1.623
$2\theta_{max}$, deg	54.96	54.96	54.96	54.96	54.96	54.96
no. of unique rflns	7952	5556	6315	9864	8807	8280
no. of obsd rflns	20681	10255	21850	33672	29718	14760
no. of parameters	347	306	299	443	434	497
GOF (F^2)	1.073	1.061	1.194	1.155	1.052	1.085
R_1[a]	0.0360	0.0335	0.0614	0.0427	0.0377	0.0304
wR_2[b]	0.0874	0.0914	0.1273	0.0918	0.0950	0.0766

[a] $R_1 = \sum||F_o| - |F_c||/\sum|F_o|$. [b] $wR_2 = \{\sum[w(F_o^2 - F_c^2)^2]/\sum w(F_o^2)^2\}^{1/2}$.

Scheme 1

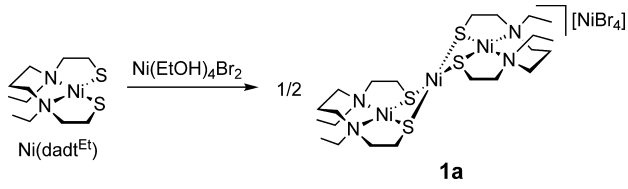

Scheme 2

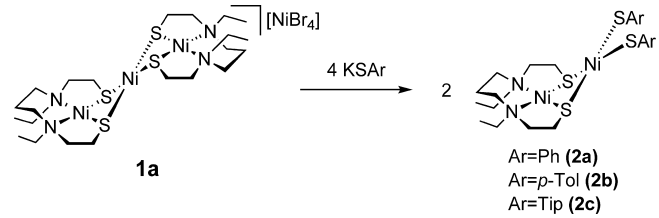

on F^2 using SHELXL-97[15] in the Rigaku/MSC CrystalStructure program package. Anisotropic refinement was applied to all non-hydrogen atoms except for the disordered atoms, and all hydrogen atoms were put at calculated positions. A phenyl group of **2a** was disordered over two positions in a 6:4 ratio. An anion of **4** was disordered over two positions in a 1:1 ratio. Additional crystallographic data are given in the Supporting Information.

Results and Discussion

Synthesis of Dinuclear Nickel Complexes Having Thiolates at the Model Ni_p Site. We chose Ni(dadt^{Et}) as a building block of dinuclear nickel complexes modeling the ACS dinuclear nickel site and examined the reaction with $NiBr_2(EtOH)_4$. When the reaction was conducted in ethanol, a dark green crystalline powder precipitated immediately. This dark green product was identified as the trinuclear nickel complex [{Ni(dadt^{Et})}$_2$Ni][$NiBr_4$] (**1a**) by X-ray structural analysis (Scheme 1), in which the trinuclear nickel cation is the same as that of [{Ni(dadt^{Et})}$_2$Ni][$NiPPh_3Cl_3$]$_2$ reported by Holm and co-workers.[7c]

Although the desired dinuclear nickel complex could not be isolated from the Ni(dadt^{Et}) + $NiBr_2(EtOH)_4$ reaction system, **1a** was found to serve as a convenient precursor for the preparation of dinuclear nickel complexes. The reactions of **1a** with a series of potassium arenethiolates in ethanol afforded Ni(dadt^{Et})Ni(SAr)$_2$ (Ar = Ph (**2a**), Ar = *p*-Tol (**2b**), Ar = Tip (**2c**)) as reddish brown precipitates, and the products were isolated in 62−91% yields based on Ni of **1a** (Scheme 2). These complexes are models for the ACS active site bearing thiolate coordinated entities on the Ni_p site and can be compared with the thiolate-bridging tetranuclear nickel complex, [{Ni(L_R-S_2N_2)}Ni(S-*p*-Tol)]$_2$[PF_6]$_2$, reported by Holm et al.[7b] The sharp ^{1}H NMR signals observed for **2a**−**c** in DMSO-d_6 are indicative of diamagnetism, which shows that both nickel centers of each dinuclear complex have a square planar geometry. The two aryl groups of each complex are equivalent, so that the molecules should have mirror symmetry. The absence of change in the ^{1}H NMR spectra of **2a**−**c** from 25 to 80 °C shows their thermal stability.

The high yields of **2a**−**c** indicate that both tetrabromonickelate (2−) and the trinuclear complex dication of **1a** must be involved in the transformation from **1a** to the dinuclear nickel complexes. Accordingly, three possible pathways can be considered for this intriguing transformation, as summarized in Scheme 3. One conceivable mechanism is the formation of {Ni(dadt^{Et})}$NiBr_2$ via a ligand redistribution process of **1a**, before any reaction with KSAr occurs (Route 1 in Scheme 3). The ^{1}H NMR spectrum and the magnetic moment estimated by Evans method[13] for **1a** in CD_3OD are indicative for the {Ni(dadt^{Et})}$NiBr_2$ formation. The magnetic moment shows considerably smaller value (μ_{eff} = 0.5 μ_B) than the expected value for the tetrahedral $[NiBr_4]^{2-}$.[16] Thus, the ^{1}H NMR signals are reasonably sharp, in which a major set of signals assignable to a dadt^{Et} ligand is different from that observed for [{Ni(dadt^{Et})}$_2$Ni][PF_6]$_2$ (**1b**) (see below). These results could

(15) Sheldrick, G. M. *SHELX97*; University of Göttingen; Göttingen, Germany, 1997.

(16) The magnetic moment for $(NEt_4)_2[NiBr_4]$ in the solid state was reported as μ_{eff} = 3.80 μ_B (298 K), see Sacconi, L.; Ciampolini, M.; Campogli, U. *Inorg. Chem.* **1965**, *4*, 407–409.

Scheme 3

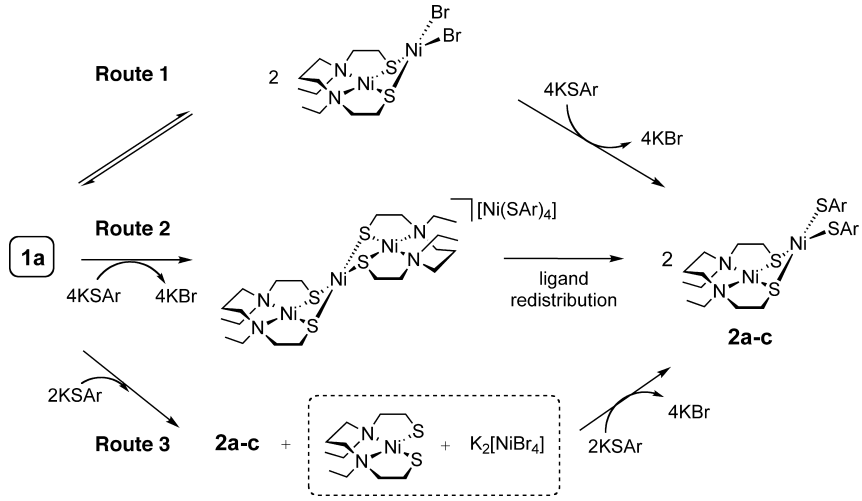

Scheme 4

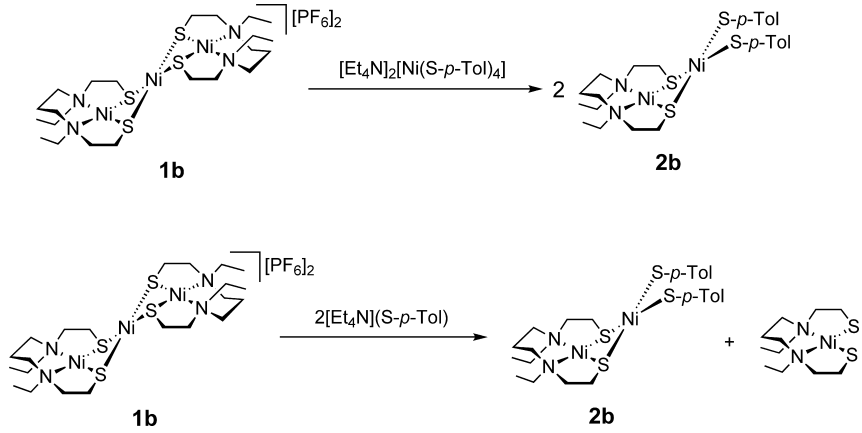

suggest that **1a** and $\{Ni(dadt^{Et})\}NiBr_2$ are in equilibrium assuming diamagnetism of $\{Ni(dadt^{Et})\}NiBr_2$, and $\{Ni(dadt^{Et})\}$-$NiBr_2$ could be a majority in CD_3OD. Another possible mechanism is that KSAr reacts first with $[NiBr_4]^{2-}$ of **1a** to generate $[\{Ni(dadt^{Et})\}_2Ni][Ni(SAr)_4]$, and then a thiolate transfer occurs from $[Ni(SAr)_4]^{2-}$ to $[\{Ni(dadt^{Et})\}_2Ni]^{2+}$ giving rise to $Ni(dadt^{Et})Ni(SAr)_2$ (Route 2). Alternatively, 2 equiv of KSAr could directly attack the trinuclear complex cation to form Ni-$(dadt^{Et})Ni(SAr)_2$, with concomitant liberation of $Ni(dadt^{Et})$ and $K_2[NiBr_4]$. Subsequently, 2 equiv of KSAr may react with $K_2[NiBr_4]$ and $Ni(dadt^{Et})$, leading to $Ni(dadt^{Et})Ni(SAr)_2$ and 4 equiv of KBr (Route 3).

To gain insight into the mechanism, $[\{Ni(dadt^{Et})\}_2Ni]$-$[PF_6]_2$ (**1b**) was synthesized by anion exchange of **1a** with 2 equiv of $NaPF_6$, and the reactions of **1b** with $[Et_4N]_2[Ni(S$-p-$Tol)_4]$ and $[Et_4N](S$-p-Tol) were examined. Upon treating **1b** with 1 equiv of $[Et_4N]_2[Ni(S$-p-$Tol)_4]$ in acetonitrile, $Ni(dadt^{Et})Ni(S$-p-$Tol)_2$ (**2b**) was obtained in 73% yield based on nickel (Scheme 4). This result clearly indicates that facile ligand redistribution occurs between $[Ni(S$-p-$Tol)_4]^{2-}$ and $[\{Ni(dadt^{Et})\}_2Ni]^{2+}$ and supports the mechanism via Route 2 in Scheme 3. On the other hand, 2 equiv of $[Et_4N](S$-p-Tol) was also found to react with **1b** in acetonitrile, from which **2b** was isolated in 96% yield on the basis of p-toluenethiolate (Scheme 4). The product was purified by extraction with CH_2Cl_2 followed by washing of the crude product with methanol. Formation of $Ni(dadt^{Et})$ was noticed in this methanol solution. Thus, p-toluenethiolate can react directly with $[\{Ni(dadt^{Et})\}_2Ni]^{2+}$ to afford the dinuclear complex **2b** and $Ni(dadt^{Et})$. This transformation corresponds to Route 3, suggesting that the mechanism involving Route 3 is as plausible as Route 2. It may be that all of the three routes in Scheme 3 are operating in the reactions of **1a** with potassium arenethiolates to give **2a**−**c** in high yields.

It should be noted here that contrary to arenethiolates, the reactions of **1a** with alkylthiolates such as ethanethiolate or t-butanethiolate did not produce the desired dinuclear complexes. These reactions led to formation of $Ni(dadt^{Et})$ and the concomitant precipitation of uncharacterizable Ni/S containing compounds, which are insoluble to common organic solvents. We attribute this to the stronger S-donor property of the alkylthiolates than those of arenethiolates and the thiolate sulfur atoms in the $Ni(dadt^{Et})$ complex, which would cause the displacement of $Ni(dadt^{Et})$ of **1a** to produce insoluble oligomeric/polymeric nickel alkylthiolates.

Synthesis of Cationic Dinuclear Nickel Complexes Having Neutral Ligands at the Model Ni_p Site. Cationic dinuclear nickel complexes ligated by ^{t}BuNC or tetramethylthiourea (tmtu) at the Ni_p site could also be synthesized from **1a**. When a methanol solution of **1a** was treated with AgOTf (4

Scheme 5

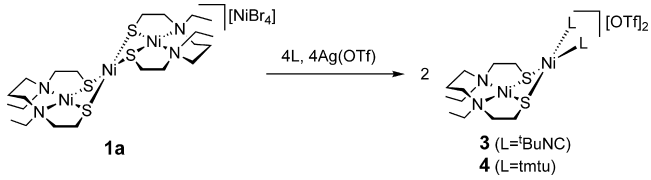

equiv) in the presence of ^{t}BuNC, the color of the solution turned from dark green to red, and [Ni(dadt^{Et})Ni(CN^{t}Bu)$_2$](OTf)$_2$ (**3**) was isolated in 64% yield as a red powder. The tmtu analogue, [Ni(dadt^{Et})Ni(tmtu)$_2$](OTf)$_2$ (**4**), was obtained in 56% yield as a dark purple powder via a similar procedure (Scheme 5). As is the case of the reactions between **1a** and potassium salts of arenethiolates, the $[NiBr_4]^{2-}$ of **1a** appears to contribute to the formation of **3** and **4**. Thus, a mechanism equivalent in Scheme 3 may be applied to the transformation from **1a** to **3** or **4**.

The structures of **3** and **4**, revealed by X-ray crystallography, show two ^{t}BuNC ligands or two tmtu ligands coordinated to the Ni_p site of the dinuclear structures, respectively. The IR spectrum of **3** shows two characteristic bands at 2228 and 2219 cm^{-1}, which are attributable to the CN stretch of ^{t}BuNC. These are significantly shifted to higher frequencies from that of free ^{t}BuNC (2136 cm^{-1}) as has been reported for other nickel(II)-isocyanide complexes.[17]

Molecular Structures and Structural Comparison with A-cluster. The structures of **1a**, **2a**, **2b**, **2c**, **3**, and **4** were elucidated by X-ray crystallography, and those of **2a**, **3**, and **4** are shown in Figures 2, 3, and 4, respectively. The structures of **2b** and **2c** are very similar to that of **2a** except for the identity of arenethiolates on Ni(2), and the structure of the trinuclear dication of **1a** has been reported[7c] (see Supporting Information). Selected bond lengths and angles of **1a**, **2a**, **2b**, **2c**, **3**, and **4** are listed in Table 2 together with the structural parameters reported for the A-clusters in ACS_{Mf}.

Both nickel centers of each complex display a square planar geometry as is common for Ni(II) complexes. The two coordination planes are folded along the μS-μS vector. The dihedral angle defined by the two Ni(μ-S)$_2$ planes in each complex falls in a relatively narrow range of 105−115°,

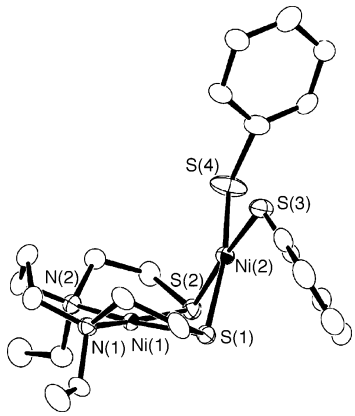

Figure 2. Oak Ridge Thermal Ellipsoid Plot (ORTEP) drawing of Ni(dadt^{Et})Ni(SPh)$_2$ (**2a**). Thermal ellipsoids are shown at 50% probability. The phenyl ring bonded to S(3) was modeled with two disordered components in a 60:40 ratio, and the major component is shown.

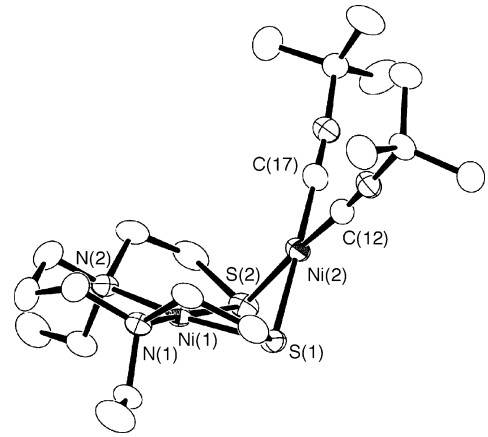

Figure 3. ORTEP drawing of the complex cation [Ni(dadt^{Et})Ni(CN^{t}Bu)$_2$]$^{2+}$ (**3**). Thermal ellipsoids are shown at 50% probability.

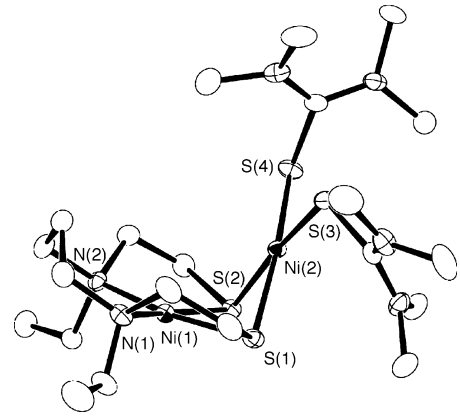

Figure 4. ORTEP drawing of the complex cation [Ni(dadt^{Et})Ni(tmtu)$_2$]$^{2+}$ (**4**). Thermal ellipsoids are shown at 50% probability.

and the Ni···Ni are consequently separated (2.718−2.830 Å). The small fold of the Ni_2S_2 quadrangles and thus shorter Ni···Ni distances compared with these for the A-cluster would be ascribed to the geometrical difference of the N_2S_2 ligands.

The bond lengths around Ni(1) are nearly identical among these model complexes and their Ni(1)-μS bonds are a little shorter than those of the A-cluster. The bond angles around Ni(1) are varied according to the lengths of the carbon chains in the N_2S_2 ligand. The dadt^{Et} ligands in these complexes show a common geometrical feature, namely, that the ethylene carbons bridging S and N, in the Ni(1)SCCN pentagons of dadt^{Et} with an envelope conformation, are all located above the Ni(1)S_2N_2 plane. The Ni(2) atom coordinates at the dadt^{Et} sulfurs also from above the Ni(1)S_2N_2 plane, probably because of a favorable interaction with the S lone pairs, in turn determined by the conformation of the dadt^{Et} ligand. A similar conformation of dadt^{Et} had been reported for [Ni(dadt^{Et})Ni(SCH$_2$CH$_2$PPh$_2$)][PF$_6$] and [Ni(dadt^{Et})-Ni(dppe)][PF$_6$]$_2$, in which the folded geometry of the Ni_2S_2 core, the square planar geometry of the nickels, and the metric parameters around the nickels also compare well with those for **2a**−**c**, **3**, and **4**.[7c,f]

Contrary to the insignificant geometrical differences at Ni(1) among models, the Ni(2)-μS bond lengths vary depending on the ligands trans to them. In particular, the Ni(2)-μS bonds of **3** are significantly shorter than **2a**−**c**

Table 2. Selected Bond Distances (Å) and Angles (deg) for **1a**, **2a**, **2b**, **2c**, **3**, **4**, and A-cluster

distance/angle	**1a**[a]	**2a**	**2b**	**2c**	**3**	**4**	A-cluster$_{Mt}$[b]
Ni(1)−N(1)	1.999	1.9919(18)	1.983(3)	1.983(2)	1.9790(18)	1.9833(14)	2.00
Ni(1)−N(2)	1.989	2.0012(19)	1.992(3)	1.9933(16)	1.9840(19)	1.989(2)	1.97
Ni(1)−S(1)	2.176	2.1648(7)	2.1613(11)	2.1623(5)	2.1636(6)	2.1606(6)	2.22
Ni(1)−S(2)	2.171	2.1716(6)	2.1723(11)	2.1712(6)	2.1666(5)	2.1651(4)	2.25
Ni(2)−S(1)	2.193	2.2437(7)	2.2449(11)	2.2604(5)	2.1919(5)	2.2247(4)	2.35
Ni(2)−S(2)	2.193	2.2258(7)	2.2255(11)	2.2381(6)	2.2062(5)	2.2166(5)	2.14
Ni(2)−L(1)[c]		2.1763(7)	2.1755(13)	2.2154(6)	1.851(2)	2.2079(7)	2.34
Ni(2)−L(2)[d]		2.1930(8)	2.1899(12)	2.1751(5)	1.848(2)	2.2008(4)	2.38
Ni(1)−Ni(2)	2.830	2.7918(5)	2.7363(6)	2.7237(3)	2.7604(5)	2.7178(3)	3.04
N(1)−Ni(1)−N(2)	101.85	101.14(7)	100.78(14)	100.20(7)	102.34(7)	101.49(7)	84
N(1)−Ni(1)−S(1)	88.68	89.30(6)	89.80(10)	90.01(4)	88.89(5)	89.61(6)	105
N(2)−Ni(1)−S(2)	88.93	89.66(5)	89.98(10)	90.11(6)	89.24(5)	89.76(4)	84
S(1)−Ni(1)−S(2)	80.04	79.57(2)	79.21(4)	79.56(2)	79.26(2)	78.68(2)	87
S(1)−Ni(2)−S(2)	79.11	76.75(2)	76.34(4)	76.10(2)	77.801(19)	76.254(19)	87
S(1)−Ni(2)−L(1)[c]	100.89	89.81(3)	91.79(4)	91.63(2)	95.28(7)	91.98(2)	106
S(2)−Ni(2)−L(2)[d]		100.40(2)	97.82(4)	103.58(2)	96.09(7)	97.65(2)	81
L(1)−Ni(2)−L(2)[c,d]		93.29(3)	94.86(4)	90.11(2)	90.81(10)	94.145(19)	86
Ni(1)S_2/Ni(2)S_2[e]	115.2	109.5	105.9	104.8	109.6	105.2	138

[a] The metric parameters are averaged between the two chelates of the Ni(dadt^{Et}) units. [b] A-cluster from *M. thermoacetica*.[3] [c] L(1) = S(3) for **2a**, **2b**, **2c**, and **4**, L(1) = C(12) for **3**, and L(1) = S for A-cluster. [d] L(2) = S(4) for **2a**, **2b**, **2c**, and **4**, L(2) = C(17) for **3**, and L(2) = X for A-cluster shown in Figure 1. [e] Dihedral angle.

which have arenethiolates, indicating the weaker trans influence of ^{t}BuNC than that of the thiolates. Since the corresponding Ni(2)-μS bonds of **4** are also shorter than **2a**−**c** but a lesser extent than **3**, tmtu is evidently a stronger donor than ^{t}BuNC. Although the Ni(2)-μS bond lengths are varied, they are all longer than the Ni(1)-μS bonds. Thus, the macrocyclic dadt^{Et} ligand is tightly bound to Ni(1). A notable difference between these models and A-cluster is found in the Ni(2)−S(1) bond distances. The model complexes have shorter Ni(2)−S(1) bond distances compared with that of the A-cluster, which may indicate the stronger trans-influence of the unidentified ligand X. The bond lengths of Ni(2)−S(3) in complex **2a**−**c** are shorter than that of A-cluster, simply because the cysteine sulfur is bridging between Ni(2) and an Fe atom of the [Fe_4S_4] cluster in the A-cluster.

Acknowledgment. This research was financially supported by Grant-in-Aids for Scientific Research (No. 18GS0207 and 18065013) from the Ministry of Education, Culture, Sports, Science, and Technology, Japan. We are grateful to Prof. Roger E. Cramer for discussions and careful reading of the manuscript.

Supporting Information Available: X-ray crystallographic data for **1a**, **2a**−**c**, **3**, and **4** are given in CIF format. This material is available free of charge via the Internet at http://pubs.acs.org.

IC801967E

(17) (a) Singleton, E.; Oosthuizen, H. E. *Adv. Organomet. Chem.* **1984**, *22*, 209. (b) Wang, R.; Groux, L. F.; Zargarian, D. *Organometallics* **2002**, *21*, 5531–5539. (c) Braun, T.; Blöcker, B.; Schorlemer, V.; Neumann, B.; Stammler, A.; Stammler, H.−G. *J. Chem. Soc., Dalton Trans.* **2002**, 2213–2218.